

OPERATION OF TARN

Yasuo Hirao  
 Institute for Nuclear Study, University of Tokyo  
 Midoricho 3-2-1, Tanashi, Tokyo 188, Japan

Summary

The construction of a Test Accumulation Ring for NUMATRON Project, TARN, was finished and the first injection test was performed successfully in August, 1979. For testing the beam accumulation technology by a combination of multiturn injection and RF stacking,  $He^{2+}$ ,  $H_2^+$  and  $H^+$  beams of 7 MeV/u were used so far. Through this work, various important technical problems for the NUMATRON were solved.

1. Introduction

Several years ago, a high-energy heavy-ion accelerator project was proposed in order to respond to many demands not only in the field of nuclear physics but also in many other fields of fundamental researches and applications, which is named NUMATRON Project.<sup>1</sup>

The energy-mass capability of the NUMATRON is shown in Fig. 1 together with those of the other machines in operation, under construction and in planning stage in the world. All of the accelerator higher than 200 MeV per nucleon consist of injector linac and synchrotron. At the design stage of this type of accelerator complex, a synchrotron with an accumulation ring is the most preferable for obtaining an expected high-intensity beam, considering present ion-source technologies and low duty factor of synchrotron. The main difficulties expected in the

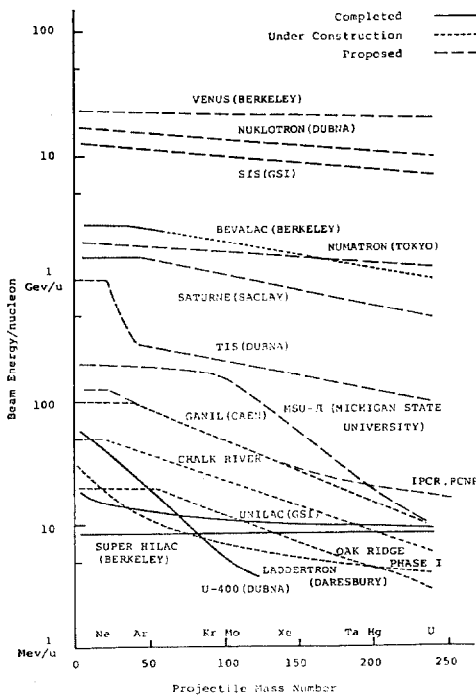


Fig. 1 mass-energy capability of heavy-ion accelerators.

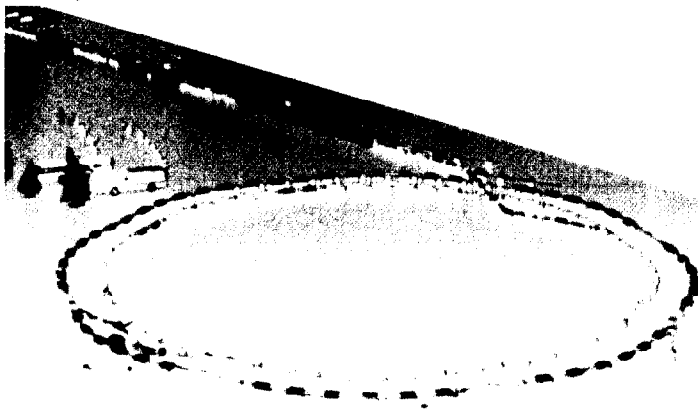


Fig. 2 1/100 scaled model of NUMATRON

construction of this type of heavy-ion machine are in the requirements for an ultrahigh vacuum in the synchrotron ring and devices for beam control by detecting a very low beam current without destruction. How to accumulate the heavy-ion beam efficiently, is also the problem to be studied carefully.

In order to investigate these problems, several preparatory works have been carried out. One of the most important achievements is the construction of a test accumulation ring of 10 m in diameter<sup>2</sup> as shown in Figs. 3 and 4. The injector cyclotron has been in operation since 1974. Ions from proton to neon, e. g.  $^{14}N^{5+}$  of 8.5 MeV/u, are injected and stacked into the TARN. The beam of  $^{14}N^{5+}$  was supposed in the design calculations. Most of the test experiments were done by use of  $He^{2+}$ . Detailed descriptions of the following sections can be found in the other papers to this conference.

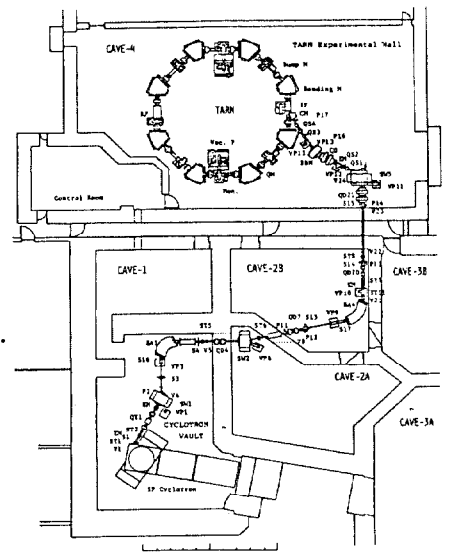


Fig. 3 Layout of TARN and beam transport system from SF Cyclotron



Fig. 4 Total view of TARN

2. Beam Transport and Injection System

The beam transport system consists of the following four sections in series from the cyclotron: momentum analysing section which gives the required momentum resolution ( $\Delta p/p \sim 1 \times 10^{-3}$ ) for the RF stacking, momentum matching section where doubly achromatic beam ( $\eta_h = 0, \eta'_h = 0$ ) is produced, dispersion-free matching section of transverse phase space to adjust the phase space diagram to the one required for the multiturn injection, and momentum matching section where the dispersion parameters are matched to the required values ( $\eta_h = 1.61 \text{ m}, \eta'_h = 0.36$ ) at the injection point of the ring. Injection system consists of C type magnet and a pair of electrostatic inflector.

Obtained transmissions from the cyclotron to the ring are 17 % and 24 % for  $\Delta p/p$  of 1/1500 and 1/1000, respectively. Measured emittances in mm·mrad are 15 for horizontal and 23 for vertical, and 12 and 16.5, after extraction from the cyclotron and in the third

section of the transport system, respectively.

### 3. Multiturn Injection

A combination of multiturn injection and RF stacking is applied to the TARN. Two pulse magnets are located upstream and downstream from the injection point along the circular orbit of the ring, which produce a distortion of closed orbit for a duration of their excitation. As the pulse fields are decreasing linearly, the beam fills up the transverse phase space of the injection orbit. In the case of using the full aperture of the ring only for multiturn injection, the maximum effective intensity corresponding to 34 turns was obtained. The injection of effective intensity of 20 turns into an optimum phase space considering the combination with RF stacking has been established.

Figure 5 shows a typical result of this case using  $\text{He}^{2+}$  beam. The upper pattern shows the time structure of the current of a kicker magnet installed in the 2nd section of the transport system for pulse shaping of the beam to a duration of  $80 \mu\text{s}$ , the middle shows of the pulse magnets for distorting the orbit and the lower shows the intensity increase of the 20 turn injection.

The number of injected particles is estimated at  $2 \times 10^8$ . From the observation of injected beam profile, measured radial width is about 35 mm and then the emittance is  $153 \text{ mm} \cdot \text{mrad}$ . The decaying curve of the lower pattern does not indicate intensity decrease, but debunching effect due to a momentum spread, because of a frequency dependence of an electrostatic beam monitor. This situation can be explained more clearly by Fig. 6. In this case, the injected beam is captured by RF field and then the upper pattern illustrates well that the injected beam intensity does not decay but oscillates at frequencies corresponding the applied RF voltage shown in the lower pattern. Observed frequency of the phase oscillation is

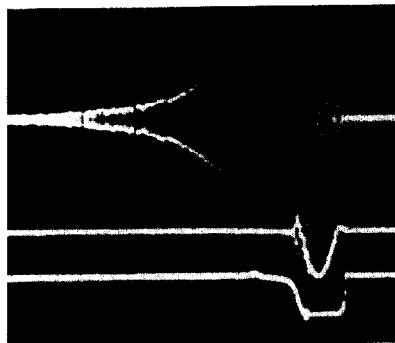


Fig. 5 Time structure of electrostatic monitor signal for the beam of 20 turn injection, upper and middle patterns show the current shapes of kicker magnet for beam pulsing and of pulse bump magnets for orbit distortion:  $100 \mu\text{s}/\text{div}$ .

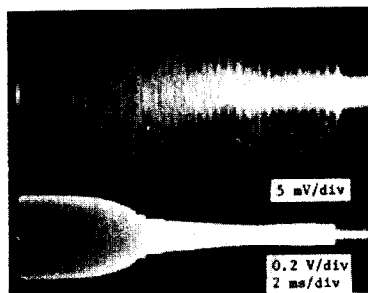


Fig. 6 Phase oscillation of the beam of 20 turn injection captured by RF field, lower shows the applied RF voltage.

Figure 7 shows the relation between the applied RF voltage and the phase oscillation frequency. The observed frequency of the phase oscillation is

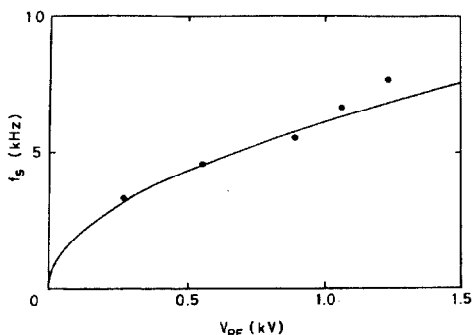


Fig. 7 Relation between RF field and Phase oscillation.

plotted as a function of the applied RF voltage as shown in Fig. 7. Fit with theoretical curve is fairly good.

### 4. RF Stacking

A procedure of RF stacking is similar to the one which is used for the proton storage at ISR, CERN.<sup>3</sup>

The RF voltage at capture process of injected beam with multiturn is determined as enough that its separatrix covers the longitudinal phase space area ( $\sim 1 \text{ rad} \cdot \text{keV}$ ) of the beam. Then the RF voltage both in the capture and acceleration processes is chosen at about 1 kV, and consequently the period of phase oscillation is about 1 ms. For a synchronous phase of  $30^\circ$ , the change rate of momentum,  $dp/Pdt$ , for synchronous particle is designed at  $1.5 \times 10^{-2} \text{ ms}^{-1}$  and fractional momentum variation from the injection orbit to the bottom of stacking region is about 4%. Then it takes 2.5 ms to move to the bottom of the stacking region. Change of revolution frequency is 30 kHz and acceleration frequency difference is 230 kHz. Momentum difference between the stacked beams at the bottom and top of the stacked region is designed at 2.5% and then the RF frequency must be changed by 150 kHz. In order to

keep synchronous phase of  $30^\circ$ , the time derivative of the frequency is of 9 kHz/ms for the voltage reduced adiabatically to 100 V. The time required for deposit is 17 ms. The expected maximum stacking number into transverse and longitudinal phase space is about 2000 turns.

The relation between the RF frequency and the radial position of the equilibrium orbit was measured by using  $\text{He}^{2+}$  beam as shown in Fig. 8. The slope of the line,  $df/dx$ , is 3.7 kHz/mm. This value is about 20% smaller than the calculated one of 4.45 kHz/mm.

The efficiency for capture and transport processes to the stacking region was also measured. The injected ions are well captured and transported at higher voltage than 130 V, and the efficiency is estimated at about 70%.

Figure 9 shows the typical result of the combination of multiturn and RF stacking. Upper pattern shows the radial beam profile of the 20 turn injection and lower pattern shows of 10 times stacking after the 20 turn injection. Total effective intensity is then of 200 turns, whereas number of revolutions may be 600, because multiturn and stacking efficiencies are 0.5 and 0.7, respectively. Number of the stacked particles is about  $1 \times 10^9$ .

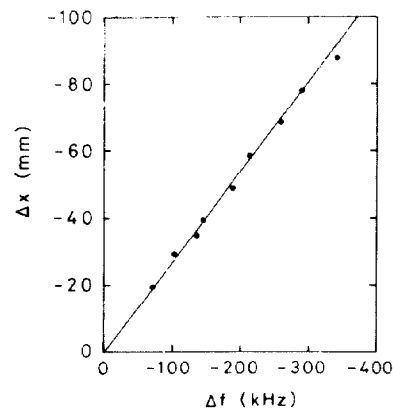


Fig. 8 Relation between frequency and radial variation of orbit.

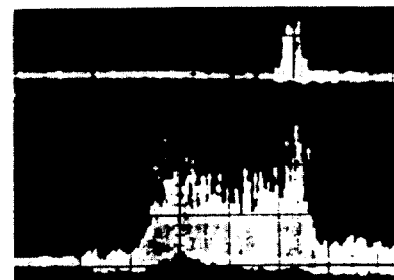


Fig. 9 Radial profiles of the beam by scintillation monitor upper: 20 turn injection, lower: combination of 20 turn injection and 10 times stacking:  $2 \text{ cm}/\text{div}$ .

### 5. Working Line Measurement

In order to tune focusing elements in the ring, the working line was measured by an RF-knockout method,

as shown in Fig. 10. Measured  $v$ -values are almost constant via momentum difference, and have a little difference with the calculated values by the computer program SYNCH as shown in Fig. 11. The chromaticity,  $\xi = \Delta v / \Delta p / p$ , is obtained to be  $\xi_x = -1.59$  and  $\xi_z = -0.47$  from these measurements. In order to control the chromaticity, two systems of 8 and 4 sextupole magnets were installed into the ring, although measurements by using these systems have not yet been done.

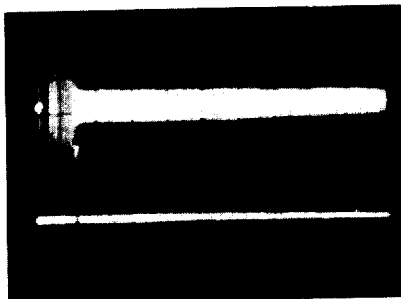


Fig. 10 RF knockout measurement, upper: electrostatic monitor signal, lower: knockout signal applied to radial direction.

Due to the low velocity of the injected particles, the transverse collective instability is expected to play a major role in limiting the number of particles that can be accumulated. Without correction of the present chromaticity, this value is about  $1 \times 10^9$ . The number already obtained may reach to a critical region of stability. By using these sextupole system, the accumulated beam will be stable up to about 25% (about  $5 \times 10^9$ ) of the design value of this injection method (about  $2 \times 10^{10}$ ). The incoherent space charge limit is the order of  $10^{12}$  and much higher than those values.

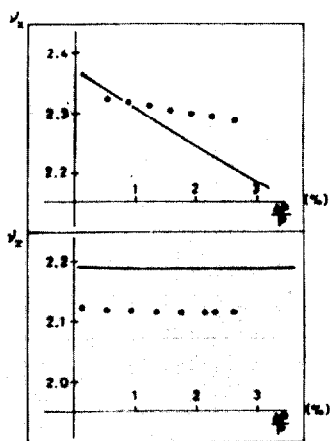


Fig. 11 Measured and calculated working lines.

#### 6. Lifetimes of the Accumulated Ions

The lifetimes of the accumulated ions were measured for  $H^+$ ,  $H_2^+$  and  $He^{2+}$ . The molecular ion was chosen as the most fragile ion. Figure 13 shows an example of the observation for  $He^{2+}$  ions of 7 MeV/u by use of radially movable plastic scintillator probe. Beam profiles of 10, 60, 180 and 300 sec after stacking processes are shown. Mean life of 250 sec is deduced from these results for the vacuum pressure ( $1 \times 10^{-10}$  Torr) during these observations. The charge exchange cross section of 7 MeV/u  $He^{2+}$  is estimated at about  $3 \times 10^{-19} \text{ cm}^2$ . The cross section for  $H_2^+$  molecular ion is also estimated at about  $4 \times 10^{-16} \text{ cm}^2$ .

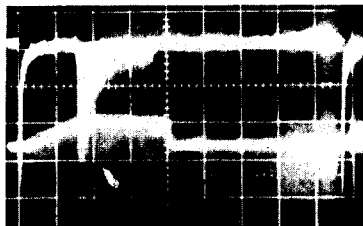


Fig. 12 Time structure of lost beam at 1/3 resonance, observed by scintillation monitor inside the chamber wall, lower: frequency variation.

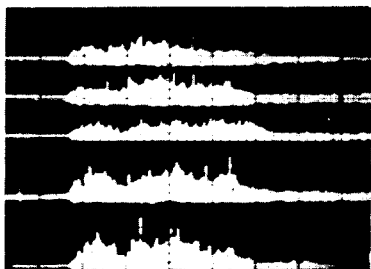


Fig. 13 Decay of the radial beam profile.

#### 7. Vacuum

Vacuum pressure lower than  $1 \times 10^{-10}$  Torr is required to achieve 90% of survival probability for various ions accumulated during a period of 1 sec. Obtained pressure is  $2 \times 10^{-11}$  Torr by cooperation of turbomolecular pumps. A small pressure increase is found as the beam is being accumulated. This amount is less than  $2 \times 10^{-11}$  Torr for the injection current of  $2 \times 10^{10}$  particles/sec of  $He^{2+}$ . The most essential procedure is thermal baking applied during pumping down process. Pumping down curve from atmospheric pressure is shown in Fig. 14. It takes about 60 hours to reach to  $1 \times 10^{-10}$  Torr and 150 hours to  $3 \times 10^{-11}$  Torr.

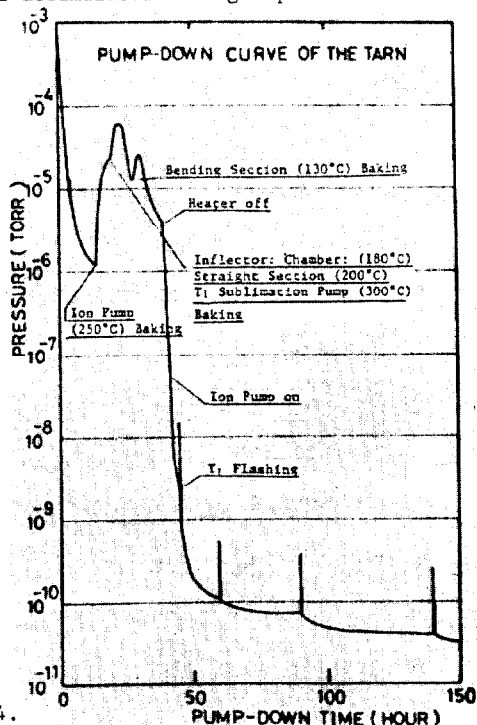


Fig. 14 Pumping down curve

#### 8. Acknowledgements

The author would like to express his sincere thanks to Dr. AL. Garren at LBL, who gave him the great contribution on beam instability. The author is very grateful to Profs. M. Sakai and K. Sugimoto for their continuous encouragements.

#### References

1. Y. Hirao et al., NUMATRON Project, IEEE Trans. NS Vol. 26, No. 3 (1979).
2. Y. Hirao et al., Test Accumulation Ring for NUMATRON Project, IEEE Trans. NS Vol. 26, No. 3 (1979).
3. W. Schnell, Proc. Conf. on High Energy Acc., Dubna (1963).